Refereed Proceedings

The 12th International Conference on Fluidization - New Horizons in Fluidization Engineering

Engineering Conferences International *Year* 2007

A Discrete Particle Simulation Study of Solids Mixing in a Pressurized Fluidized Bed

Willem Godlieb* Niels G. Deen†

J.A.M. Kuipers‡

*University of Twente, W.Godlieb@utwente.nl

†University of Twente, N.G.Deen@utwente.nl

‡University of Twente, j.a.m.kuipers@utwente.nl

A DISCRETE PARTICLE SIMULATION STUDY OF SOLIDS MIXING IN A PRESSURIZED FLUIDIZED BED

W. Godlieb, N.G. Deen*, J.A.M. Kuipers
University of Twente, Faculty of Science and Technology,
P.O. Box 217, NL-7500 AE Enschede, The Netherlands and
Dutch Polymer Institute, PO Box 902, 5600 AX Eindhoven, The Netherlands;
* Corresponding author, Tel. +31 53 489 4138, Fax +31 53 489 2882, E-mail: N.G.Deen@utwente.nl

ABSTRACT

A fluidized bed containing polymeric particles is investigated using a state-of-the-art soft-sphere discrete particle model (DPM). The pressure dependency of particle mixing, flow patterns and bubble behaviour are analysed. It is found that with increasing pressure a less distinct bubble-emulsion structure and improved solids mixing can be observed.

Keywords: high pressure fluidization, fluidized bed, discrete particle model, solids mixing.

INTRODUCTION

Polyethylene is the type of plastic with the highest production capacity in the world, which is a result of the availability of a flexible and efficient fluidized-bed-based technology using a fine catalyst. Despite decades of research, this process is not sufficiently well understood.
One of the important aspects of the fluidized bed production process is the operating pressure, which has a profound influence on the fluidization behaviour. The objective of this work is to gain insight in the fluidization behaviour of the polyethylene particles at elevated pressure, using sophisticated state-of-the-art CFD models. Several groups have reported experimental investigations of pressurized fluidized beds such as, Chan et al. (1), Sidorenko & Rhodes (2), Olowson & Almstedt (3), (4), (5), Wiman & Almstedt (6). They reported various pressure-dependent relations for gas-particle drag, bubble properties, minimum fluidization velocity, and minimum bubbling velocity.
Only recently detailed computational models have been used to study pressurized fluidized beds. Li & Kuipers (7) performed 2D discrete particle simulations. They found a less distinct bubble-emulsion structure which they attributed to the drag influence related to the competition between gas-particle and particle-particle interaction.
In a recent paper Godlieb et al. (8) we used a full 3D discrete particle model to study the effect of the operating pressure on the bubble characteristics and bed dynamics. It was found that the bubble size reduces as the pressure is increased.

The 12th International Conference on Fluidization - New Horizons in Fluidization Engineering, Art. 92 [2007]

In this work we extend the preceding work with the aid of discrete particle simulations to obtain further qualitative and quantitative knowledge on the pressure dependence of the bubble emulsion structure and solids mixing properties. Contrary to the work of Li & Kuipers (7), the simulations are carried out in full 3D, while employing a sufficiently large calculation domain.

.

GOVERNING EQUATIONS

The discrete particle model (DPM) is an Euler-Lagrange model, which was originally developed by Hoomans et al. (9). In the DPM every particle is individually tracked while accounting for particle-particle and particle-wall collisions. In the DPM the gas phase hydrodynamics are described by the Navier-Stokes equations:

$$\begin{aligned} &\frac{\partial}{\partial t}(\varepsilon_g \rho_g) + \nabla \cdot (\varepsilon_g \rho_g \overline{u}_g) = 0 \\ &\frac{\partial}{\partial t}(\varepsilon_g \rho_g \overline{u}_g) + \nabla \cdot (\varepsilon_g \rho_g \overline{u}_g \overline{u}_g) = -\varepsilon_g \nabla \rho_g - \nabla \cdot (\varepsilon_g \overline{\overline{\tau}}_g) - \overline{S}_p + \varepsilon_g \rho_g \overline{g} \end{aligned} \tag{1}$$

where $\overline{u}_g$ is the gas velocity and $\overline{\overline{\tau}}_g$ represents the gas phase stress tensor. The sink term $\overline{S}_p$, represents the drag force exerted on the particles:

$$\overline{S}_p = \frac{1}{V_{cell}} \int_{V_{cell}} \sum_{i=0}^{Npart} \frac{V_i \beta}{1-\varepsilon_g} \left(\overline{u}_g - \overline{v}_i\right) D\left(\overline{r} - \overline{r}_i\right) dV \tag{2}$$

The distribution function $D\left(\overline{r} - \overline{r}_i\right)$ is a discrete representation of a Dirac delta function that distributes the reaction force acting on the gas to the Eulerian grid via a volume-weighing technique. The inter-phase momentum transfer coefficient, β describes the drag of the gas-phase acting on the particles. The Ergun (10) and Wen & Yu (11) equations are commonly used to obtain expressions for β. However, we use the closure relation derived by Koch & Hill (12) based on lattice Boltzmann simulations, because, contrary to the Ergun and Wen & Yu relations, it has no discontinuities at high Reynolds numbers and shows good agreement with experimental data as reported by Link et al. (13) and Bokkers et al. (14).
The motion of every individual particle *i* in the system is calculated from Newtons' law:

$$m_i \frac{d\overline{v}_i}{dt} = -V_i \nabla p + \frac{V_i \beta}{\varepsilon_s} \left(\overline{u} - \overline{v}_i\right) + m_i \overline{g} + F_i^{pp} + F_i^{pw} \tag{3}$$

where the forces on the right hand side are, respectively due to the far field pressure gradient, drag, gravity, particle-particle interaction and particle-wall interaction. The contact forces are caused by collisions with other particles or confining walls and are described with a soft-sphere approach. For detailed information we want to refer to Deen et al. (15) and Van der Hoef et al. (16).

SIMULATION SETTINGS

To investigate the pressure effect on several fluidization properties five full three dimensional DPM simulations at 1, 2, 4, 8 and 16 bar were performed. The system properties and operating conditions are specified in Tables 1 and 2 respectively.

Property	symbol	value	unit	
system width	X	0.025	m	(20 cells)
system depth	Y	0.025	m	(20 cells)
system height	Z	0.1	m	(80 cells)
time step	dt	$1.0 \cdot 10^{-4}$	s	
total time	t	10	s	
number of particles	N_{part}	$2.86 \cdot 10^{5}$	-	
particle diameter	r_p	0.5	mm	
normal spring stiffness	k_n	200	N/m	
coefficient of normal restitution	e_n	0.8	-	
coefficient of tangential restitution	e_t	0.6	-	
particle density	ρ	925	kg/m^3	
friction coefficient	μ	0.1	-	

Table 1: Settings for all five simulations.

The coefficients of restitution and the friction coefficients used in the simulations were measured according to the method described by Kharaz et al. (17). No-slip boundary conditions were used at the walls.

In order to enable a fair comparison between the simulations, a constant excess velocity (i.e. superficial gas velocity minus minimum fluidisation velocity) of 0.177 m/s was applied.

P (bar)	u_{mf} (m/s)	u_{gas} (m/s)
1	0.088	0.265
2	0.084	0.261
4	0.077	0.253
8	0.067	0.244
16	0.056	0.233

Table 2: Superficial gas velocities for the 3D simulations.

The 12th International Conference on Fluidization - New Horizons in Fluidization Engineering, Art. 92 [2007]

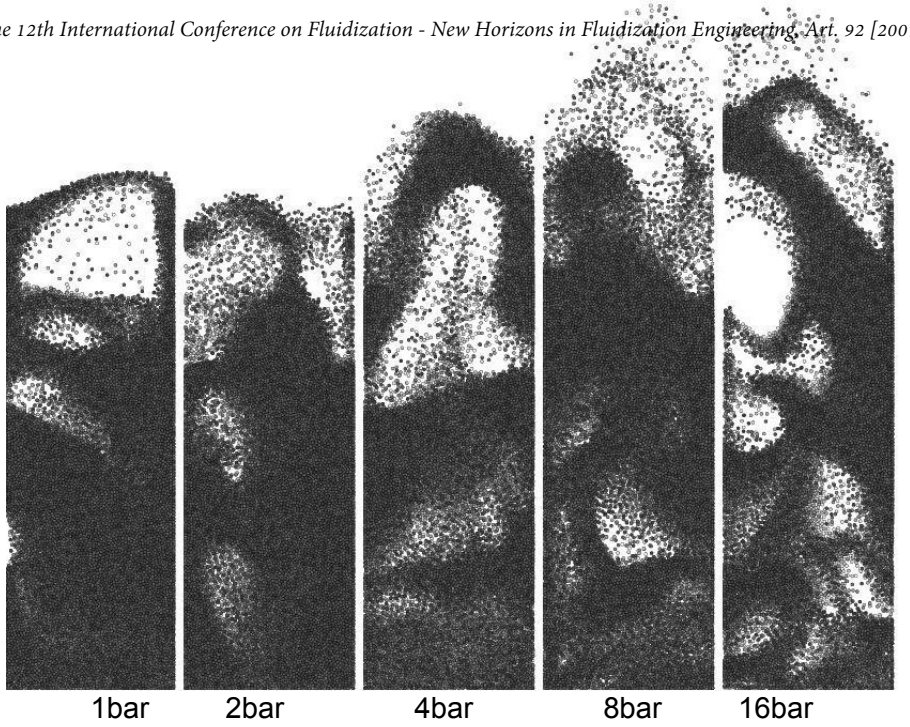

Figure 1: Snapshots of particle positions of a slice of the bed with a depth of two cells at operating pressures of 1, 2, 4, 8 and 16 bar.

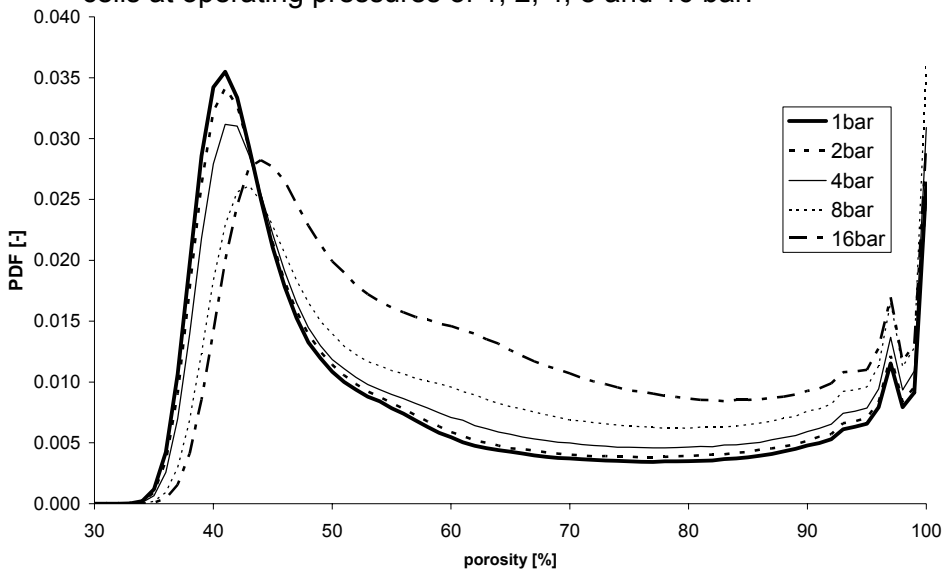

Figure 2: PDFs of time-averaged porosity distribution at operating pressures 1, 2, 4, 8 and 16 bar.

RESULTS

In this section we will discuss the results of simulation cases introduced in the previous section, where we will focus on porosity distributions and solids mixing.
Snapshots of the particles positions are shown in Figure 1. It can be observed that the bed structure is dependent on pressure. That is, at atmospheric conditions bubbles are large and contain fewer particles, whereas at elevated pressure more

and smaller bubbles are formed, which contain more particles. In order to see the effects of the pressure on the heterogeneity of the bed in a more quantitative sense, the PDFs of the time-averaged porosity distributions are shown in Figure 2.
Around a porosity of 40% - 45% we see a clear peak representing the emulsion phase. Note that at maximum packing the porosity is about 26% and random packing the porosity is 36%. Above 95% we see two peaks caused by the presence of bubbles. An intermediate area with porosities between 45% and 90% is located around bubbles or in developing or collapsing bubbles.
It is clear that the emulsion phase becomes less dense with increasing pressure, as the peak moves from 40% at 2 bar to 45% at 16 bar. Furthermore it can be observed that the intermediate region becomes more dominant with increasing pressure. Additional confirmation of the pressure effect on the bubble behaviour can be found in one of our earlier works (Godlieb et al. (8)).
Solids mixing has been investigated by several researchers such as Finnie et al. (18) and Van Puyvelde (19). In both works entropy mixing models are used to show micro mixing of the particles. In this work we look at the macro scale mixing behaviour of the entire bed and neglect the micro effects. To this end, half of the particles are given a colour and the average position of all particles is monitored. The mixing behaviour is investigated in both the vertical and horizontal directions and will now be explained for the vertical direction only. The analysis in the horizontal direction is analogous. In the first step of the algorithm, the vertical positions of all particles are sorted to determine the median height. Subsequently the lower half of the particles is coloured white, while the upper half is coloured

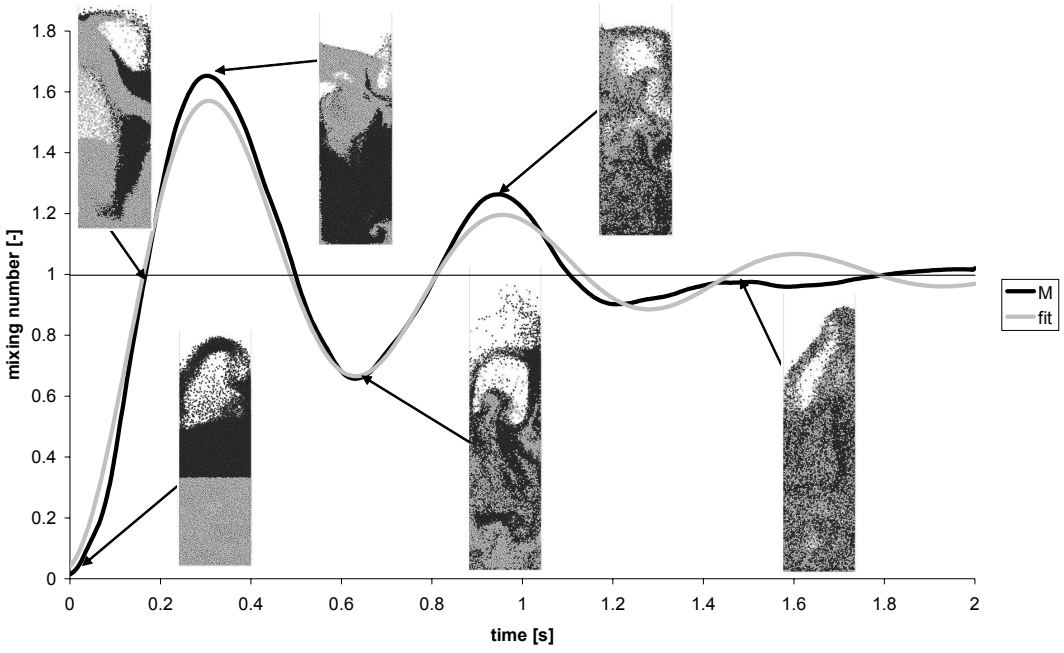

Figure 3: Vertical mixing number versus time at an operating pressure of 1 bar. Images of the particles present in a slice in the centre of the bed are shown as well.

black. For each time step the average height of the white particles can be calculated and normalised with the average height of all particles:

The 12th International Conference on Fluidization - New Horizons in Fluidization Engineering, Art. 92 [2007]

$$\overline{x}_{i,white} = \frac{\frac{1}{N_{white}} \sum_{p \in white} x_{p,i}}{\frac{1}{N_{all}} \sum_{p \in all} x_{p,i}} \tag{4}$$

where $\overline{x}_{i,white}$ is the normalised average position of the white particles in the i[th] direction. Notice that initially $\overline{x}_{i,white}$ is 0.5 and when fully mixed it is 1.0. We now define the mixing number as follows:

$$M_i = 2 \cdot (\overline{x}_{i,white} - 0.5) \tag{5}$$

which means that for M = 0 is fully segregated and for M = 1 the bed is fully mixed. Because of the circulation patterns of the particles in the bed the mixing number can exceed 1, as can be seen in Figure 3, which shows the mixing number for P = 1 bar. Although M = 1 at 0.17 seconds the bed is not fully mixed. At 0.31 seconds the colour pattern has been more or less inverted due to the bed circulation patterns. Eventually, after about 1.8 seconds the bed is almost entirely mixed.

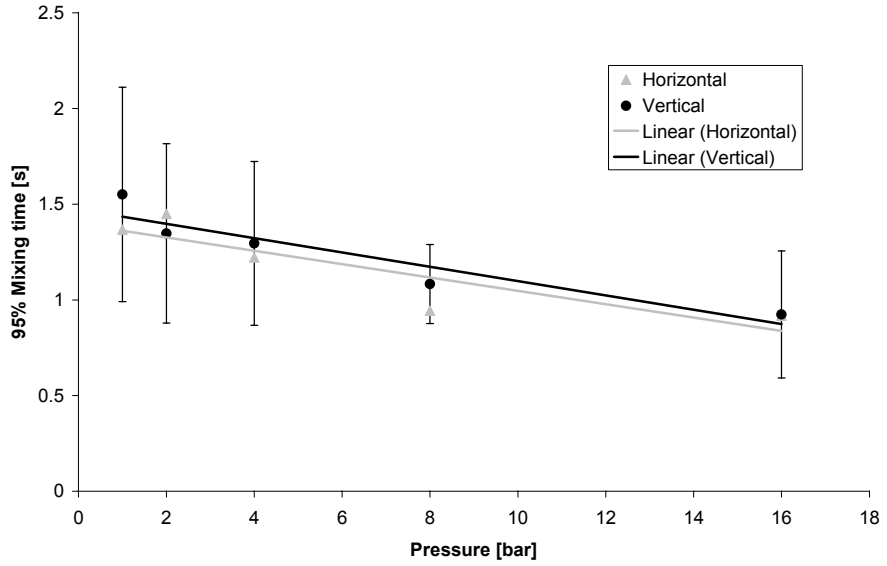

Figure 4: Horizontal and vertical 95% mixing time for different operating pressures. The error margins are twice the standard deviation of the eight analysis periods.

Since the mixing number is oscillating around 1, it is hard to determine a mixing time; therefore the curve is fitted with a damped harmonic oscillator:

$$M_{i,fit} = 1 - (Ae^{-\gamma t} \cos(\omega t)) \tag{6}$$

A, γ and ω, are the amplitude, the damping coefficient and period respectively. Each of these coefficients is fitted using a least square method. The fit as shown in Figure

3 accurately follows the trend of the curve. From this fit we can calculate the mixing time at which the bed is 95% mixed:

$$t_{95\%} = \frac{-1}{\gamma} \ln\left(\frac{1-0.95}{A}\right) \tag{7}$$

For each of the simulations we determined the mixing time for eight different analysis periods that are part of the entire simulation time: 1-3 s, 2-4 s, 3-5 s, 4-6 s, 5-7 s, 6-8 s, 7-9 s and 8-10 s. In order to prevent start-up effects from influencing the results the first second of the simulation was excluded from the analysis. From Figure 4 we observe that mixing improves with increasing pressure and the results are similar for vertical and horizontal directions.

DISCUSSION AND CONCLUSIONS

In this work, we developed a method for determining the mixing time, based on the change in the average positions of the particles. The mixing time is decreasing with increasing operating pressure. Vertical and horizontal mixing rates are similar. It is observed that the operating pressure influences the mixing rate in two ways: via the bubbles and via dense phase. From animations of the DPM results we noticed that the bubbles move more chaotically at elevated pressure, which also enhances the rate of solids mixing.

When the pressure is increased, the emulsion phase becomes less dense, creating more free space around the individual particles. Consequently the particles have a larger degree of freedom to mix. A better understanding of these phenomena requires further investigation and will be part of our future work.

In the current investigation we find that the mixing times in the horizontal and vertical directions are of the same order, irrespective of the operating pressure.

ACKNOWLEDGEMENTS

This work is part of the Research Programme of the Dutch Polymer Institute (DPI) as project number #547.

REFERENCES

1. Chan, I.H., Sishtla, C., & Knowlton, T.M. The effect of pressure on bubble parameters in gas-fluidized beds. *Powder Technology*, 53(3), 217-235(1987).
2. Sidorenko, I. & Rhodes, M.J. Influence of pressure on fluidization properties. *Powder Technology*, 141(1-2), 137-154(2004).
3. Olowson, P.A. & Almstedt, A.E. Influence of pressure and fluidization velocity on the bubble behaviour and gas flow distribution in a fluidized bed. *Chemical Engineering Science*, 45(7), 1733-1741(1990).
4. Olowson, P.A. & Almstedt, A.E. Influence of pressure on the minimum fluidization velocity. *Chemical Engineering Science*, 46(2), 637-640(1991).
5. Olowson, P.A. & Almstedt, A.E. Hydrodynamics of a bubbling fluidized bed: Influence of pressure and fluidization velocity in terms of drag force. *Chemical Engineering Science*, 47(2), 357-366(1992).
6. Wiman, J. & Almstedt, A.E. Influence of pressure, fluidization velocity and particle size on the hydrodynamics of a freely bubbling fluidized bed. *Chemical Engineering Science*, 53(12), 2167-2176(1998).

7. Li, J. & Kuipers, J.A.M. On the origin of heterogeneous structure in dense gas-solid flows. *Chemical Engineering Science*, 60(5), 1251-1265(2005).
8. Godlieb, W., Deen, N.G., & Kuipers, J.A.M. (2006). Discrete particle simulations of high pressure fluidization. In *CHISA 17th International Congress Of Chemical And Process Engineering*, Prague - Czech Republic.
9. Hoomans, B.P.B., Kuipers, J.A.M., Briels, W.J., & van Swaaij, W.P.M. Discrete particle simulation of bubble and slug formation in a two-dimensional gas-fluidised bed: A hard-sphere approach. *Chemical Engineering Science*, 51(1), 99-118(1996).
10. Ergun, S. Fluid flow through packed columns. *Chemical Engineering Progress*, 48, 89-94(1952).
11. Wen, Y.C. & Yu, Y.H. Mechanics of fluidization. *Chemical Engineering Progress Symposium*, 62, 100-111(1966).
12. Koch, D.L. & Hill, R.J. Inertial effects in suspension and porous-media flows. *Annual Review of Fluid Mechanics*, 33(1), 619-647(2001).
13. Link, J.M., Cuypers, L.A., Deen, N.G., & Kuipers, J.A.M. Flow regimes in a spout-fluid bed: A combined experimental and simulation study. *Chemical Engineering Science*, 60(13), 3425-3442(2005).
14. Bokkers, G.A., van Sint Annaland, M., & Kuipers, J.A.M. Mixing and segregation in a bidisperse gas-solid fluidised bed: A numerical and experimental study. *Powder Technology*, 140(3), 176-186(2004).
15. Deen, N.G., Annaland, M.V.S., & Kuipers, J.A.M. Detailed computational and experimental fluid dynamics of fluidized beds. *Applied Mathematical Modelling*, 30(11), 1459-1471(2006).
16. Van der Hoef, M.A., Ye, M., van Sint Annaland, M., Andrews IV, A.T., Sundaresan, S., & Kuipers, J.A.M. Multi-scale modeling of gas-fluidized beds. *Adv. Chem. Eng*, in press., (2006).
17. Kharaz, A.H., Gorham, D.A., & Salman, A.D. Accurate measurement of particle impact parameters. *Measurement Science and Technology*, 10(1), 31(1999).
18. Finnie, G.J., Kruyt, N.P., Ye, M., Zeilstra, C., & Kuipers, J.A.M. Longitudinal and transverse mixing in rotary kilns: A discrete element method approach. *Chemical Engineering Science*, 60(15), 4083-4091(2005).
19. Van Puyvelde, D.R. Comparison of discrete elemental modelling to experimental data regarding mixing of solids in the transverse direction of a rotating kiln. *Chemical Engineering Science*, 61(13), 4462-4465(2006).